Pressure dependence of the structure of liquid InAs up to 13 GPa

T Hattori[1], T Kinoshita, T Narushima and K Tsuji

Department of Physics, Keio University, Yokohama 223-8522, Japan

E-mail: takanori@phys.keio.ac.jp (T Hattori)

Abstract
The structure of liquid InAs has been investigated at pressures up to 13 GPa by means of synchrotron x-ray diffraction. The results show a change of the contraction behaviour. Below 9 GPa, liquid InAs contracts almost uniformly, which is inferred from there being no remarkable pressure-induced change in the shapes of the structure factor, $S(Q)$, and the pair distribution function, $g(r)$, and in the coordination number. Above 9 GPa, the liquid contracts nonuniformly, which is inferred from the gradual change in the shapes of $S(Q)$ and $g(r)$ and the continuous increase of the coordination number from 6 to 7. The analysis of $g(r)$ shows that liquid InAs consists of β-Sn-like and bcc-like local structures, which do not appear in crystalline InAs, throughout the whole pressure region up to 13 GPa. The fraction of the high-pressure form (bcc-like local structure) increases above 9 GPa, while it is almost constant below 9 GPa. These findings suggest that liquid InAs transforms from the state consisting of a relatively stable local structure into a transient state in which the local structure continuously changes with pressure.

1. Introduction

The pressure-induced changes of tetrahedrally bonded materials have attracted much attention due to the drastic change in the electric properties as well as the change in the atomic arrangements [1]. Recent studies on the liquids of the tetrahedrally bonded materials suggested that the pressure-induced changes of the local structures are considerably different for liquid and crystalline states [2–9]. For example, the local structures of liquid Ge and liquid III–V compounds continuously change as the pressure is raised, while those of the crystalline phases change abruptly at each transition pressure. Revealing the origin of the difference in pressure-induced changes is very interesting as regards knowing the effect of the disorder in the atomic arrangement on the pressure-induced structural changes.

---

[1] Author to whom any correspondence should be addressed.

Furthermore, the effects of the ionic character in the chemical bonds on the local structure and the pressure-induced changes are also interesting. In crystalline states, the tetrahedrally bonded materials show different pressure-induced structural changes depending on the ionic character in the chemical bonds [1]. For example, the materials with the smaller ionic character transform from the diamond/zinc-blende structure into metallic β-Sn structure or the related orthorhombic *Imma* structure at tens of gigapascals, while those with the larger ionic character transform from the zinc-blende structure into the metallic rock-salt structure and/or the related orthorhombic *Cmcm* structure. Since the liquids of the tetrahedrally bonded materials preserve the covalent and/or ionic character in the chemical bonds (even though they show metallic behaviour in the electric properties), the pressure-induced structural changes of the liquid phases are also considered to be affected by the ionic character. However, the effect has not been investigated so far. On the basis of these motivations, we have investigated the structure of liquid InAs, which has a relatively large ionic character (a Phillips ionicity of $f_i = 0.357$ [10]) among III–V compounds, using a high-pressure and high-temperature synchrotron x-ray diffraction technique.

The following high-pressure phases are reported in crystalline InAs. The zinc-blende structure transforms into the rock-salt structure at about 7 GPa [11–13], and then into the distorted rock-salt structure with the space group *Cmcm* at 9 GPa through an unidentified intermediate phase [14]. With increasing temperature at ambient pressure, the zinc-blende-type InAs melts at 1215 K and this is accompanied with a significant volume decrease. This is consistent with the negative slope of the melting curve in the $P-T$ phase diagram [15].

2. Experiment

The structure of liquid InAs was investigated by an energy-dispersive x-ray diffraction (EDX) method using a synchrotron radiation source. High-pressure and high-temperature conditions are generated by a multi-anvil high-pressure apparatus, MAX80 [16], installed in PF-AR, KEK. The experimental set-up is the same as those described in Hattori *et al* [7]. Reagent-grade InAs with a purity of 99.999% was used as the sample. To avoid too heavy absorption of x-rays by the sample, the sample was diluted by rock-salt so that μt became equal to 2 for the x-ray energy of 40 keV, where μ is the average x-ray absorption coefficient and t is the sample thickness. The cell assemblies used in the high-pressure experiments and the detailed experimental procedures were the same as those described in Hattori *et al* [7]. The experimental $P-T$ conditions and the phase boundaries determined in this study are shown in figure 1. Pressure was determined from the lattice parameters of rock-salt [17]. Temperature was determined from the power applied to the heater. The relation between the applied power and the generated temperature was calibrated beforehand. The uncertainties of the pressure and temperature were 0.7 GPa and 100 K, respectively. The total $S(Q)$ and $g(r)$ of liquid InAs were obtained by the same procedure as those described in [7], where the definitions of the total $S(Q)$ and $g(r)$ are based on Faber and Ziman [18]. The structural information is summarized in table 1.

3. Results

Figure 2 shows $S(Q)$ for liquid InAs at high pressures. Throughout the whole pressure region of the present study, the characteristic hump is observed on the high-Q side of the first peak. This suggests the existence of an anisotropic local structure in liquid InAs. Near ambient pressure ($P \approx 2.6$ GPa), the height of the first peak is much smaller than that for a simple
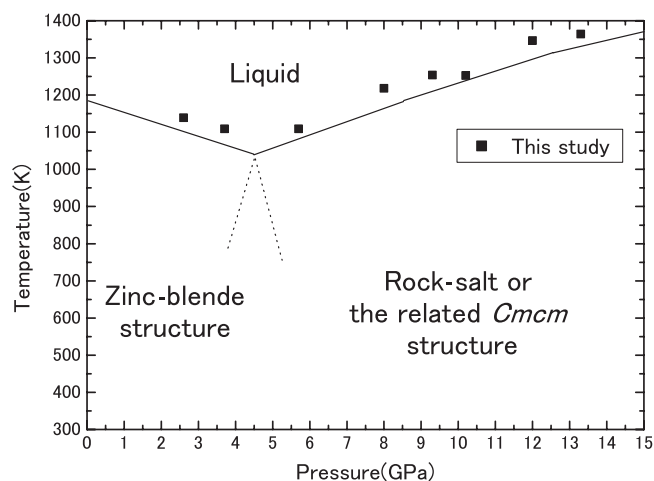
Figure 1. The $P-T$ phase diagram of InAs and the experimental conditions in this study. Phase boundaries are determined in this study. The dotted lines mean the uncertainty of the phase boundary due to the kinetic effect.

Table 1. Structural information on liquid InAs at high pressures.

P (GPa)	Q_1 (Å^{-1})	Q_2 (Å^{-1})	Q_2/Q_1	r_1 (Å)	r_2 (Å)	r_2/r_1
2.3	2.32	4.91	2.11	2.87	6.05	2.11
3.7	2.34	4.93	2.11	2.86	5.99	2.10
5.7	2.38	4.93	2.07	2.83	5.87	2.07
8.0	2.40	4.98	2.08	2.79	5.82	2.08
9.3	2.40	5.00	2.08	2.79	5.80	2.08
10.2	2.41	5.00	2.08	2.78	5.76	2.07
12.0	2.45	5.07	2.07	2.79	5.70	2.04
13.3	2.46	5.09	2.07	2.78	5.70	2.05

liquid. The ratio of the wavenumbers of the first and second peaks, Q_2/Q_1 (≈ 2.11), is much larger than that for a simple liquid (≈ 1.86 [19]). These features are completely different from those for a simple liquid. On the other hand, these are commonly observed in the liquids of the tetrahedrally bonded materials [20, 2, 3, 5–9, 21]. These results imply that the local structure of liquid InAs is not a simple one, but is a complex one as observed in the liquids of the tetrahedrally bonded materials. Since the anisotropic local structures in the liquids of the tetrahedrally bonded materials originate from the covalent character in the chemical bonds, liquid InAs is expected to have a covalent character to some extent.

As the pressure is raised, the shape of the profile of $S(Q)$ changes anisotropically. For example, the position of the first peak markedly shifts toward a high Q value, while those of the second and third peaks shift only slightly. The height of the first peak continuously increases with increasing pressure, while those of the second and third peaks do not show a marked increase. Simultaneously, the position of the hump slightly shifts toward a low Q value. If the liquid contracts uniformly, $S(Q)$ only shifts toward a high Q value without the shape of the profile changing. The observed changes in $S(Q)$ suggest that liquid InAs contracts nonuniformly and the local structure changes with increasing pressure.

Figure 3 shows $g(r)$ for liquid InAs at high pressures. Throughout the whole pressure region of the present study, the characteristic hump is observed on the large-r side of the first
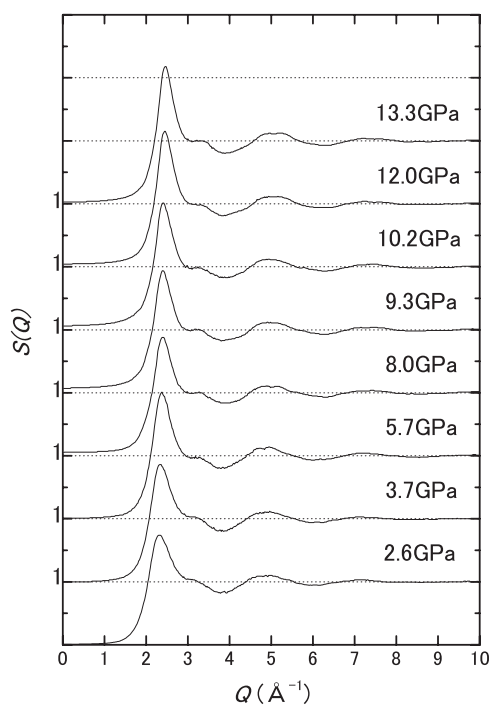
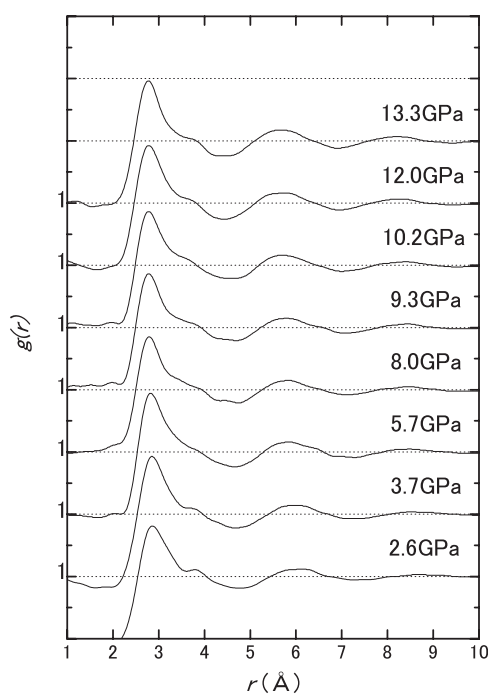**Figure 2.** $S(Q)$ for liquid InAs at high pressures.

Figure 3. $g(r)$ for liquid InAs at high pressures.

peak. Near ambient pressure ($P = 2.6$ GPa), the height of the first peak in $g(r)$ is much smaller than that for a simple liquid (≈ 3 [19]). The ratio of the positions of the first and seconds peaks, r_2/r_1 (≈ 2.11), is much larger than that for a simple liquid (≈ 1.84–1.90 [19]). These features are completely different to those for a simple liquid, but are similar to those observed in the liquids of tetrahedrally bonded materials [2–7, 25, 8, 9, 20, 21]. This supports the idea that the local structure of liquid InAs is not a simple one, but is a complex one which is similar to those of the liquids of the tetrahedrally bonded materials. As the pressure is raised, the shape of the profile of $g(r)$ changes anisotropically. For example, the positions of the second and third peaks shift toward a small-r value markedly, while that of the first peak does not shift so much. Simultaneously, the height of the hump becomes smaller. If the liquid contracts uniformly, the profile of $g(r)$ only shifts toward a small-r value without the shape changing. The observed changes suggest that the liquid contracts nonuniformly and that the local structure changes with increasing pressure.

To elucidate the contraction process of liquid InAs, the positions of the first, second and third peaks in $g(r)$ at high pressures are shown against the average interatomic distance which is defined by the cube root of the volume per atom (figure 4). Here, each value is normalized by the respective value at ambient pressure. The value at ambient pressure is estimated by the extrapolation of the data below 5.7 GPa. For comparison, the line for the uniform contraction model is also shown. The result shows that the pressure dependence of the position for the first peak changes at about 9 GPa. In the low-pressure region, the position changes markedly with increasing pressure, while in the higher-pressure region it does not change so much in spite of the volume contraction. We can also find that the pressure dependence of the first peak is almost along the line for the uniform contraction in the lower-pressure region, although it
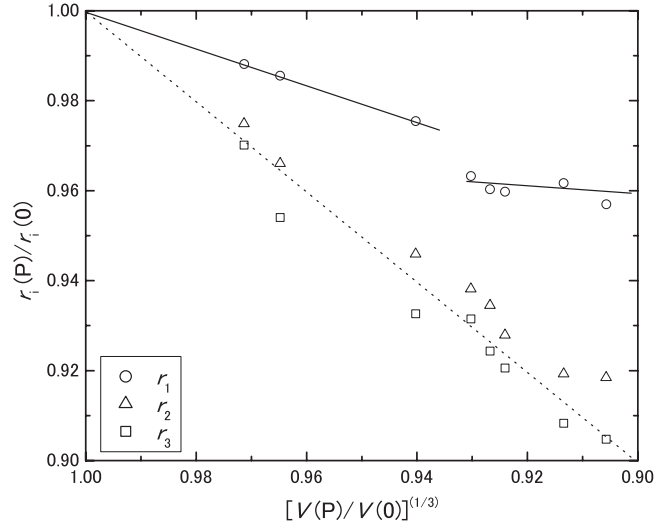
Figure 4. The pressure dependence of the peak positions against the average interatomic distance. Each value is normalized by the respective value at ambient pressure. The dotted line is for a uniform contraction model. The thin lines are only a guide for the eye.

has a small deviation. These findings suggest that the liquid contracts almost uniformly below 9 GPa, while it contracts nonuniformly above 9 GPa.

To reveal the pressure-induced change of the local structure, the pressure dependence of the coordination number is investigated. The coordination number is calculated from the radial distribution function, RDF, on the basis of the following equation:

$$\mathrm{CN} = 2 \int_{r_0}^{r_{\max}} 4\pi r^2 \rho_0 g(r) \, \mathrm{d}r. \tag{1}$$

Here, r_0 is the low-r limit of the first peak in RDF and $r_{\max}$ is the r value at the top of the first peak in RDF. ρ_0 is the average atomic density. In the present study, an exact coordination number cannot be determined because the partial pair distribution functions, $g_{\mathrm{In-In}}$, $g_{\mathrm{As-As}}$, $g_{\mathrm{In-As}}$ cannot be obtained by a conventional EDX method. In this case, the coordination number depends on the assumed model for the chemical short-range order (see [7]). Therefore, the coordination numbers for a disordered model ($g_{\mathrm{In-In}} = g_{\mathrm{As-As}} = g_{\mathrm{In-As}}$) and for an ordered model ($g_{\mathrm{In-In}} = g_{\mathrm{As-As}} = 0$ in the first coordination shell) are calculated. Since the degree of the ordering would be intermediate between these extreme cases, the coordination number would become an intermediate value between the values for these models. The coordination numbers for both models are shown in figure 5. The uncertainty is estimated from the scatter of the data.

Near ambient pressure ($P \approx 2.6$ GPa), the coordination number is about 6 both for a disordered and for an ordered model. On application of pressure up to about 9 GPa, the coordination number is constant or slightly decreases. On further compression up to 13 GPa, the coordination number significantly increases up to about 7. This suggests that the local structure does not change so much below 9 GPa, and it starts to change into a highly coordinated form above 9 GPa. This pressure dependence is consistent with the aforementioned pressure dependences of the peak positions. These results imply that the liquid has a relatively stable local structure, which is not changed by the application of pressure, in the pressure region below 9 GPa.
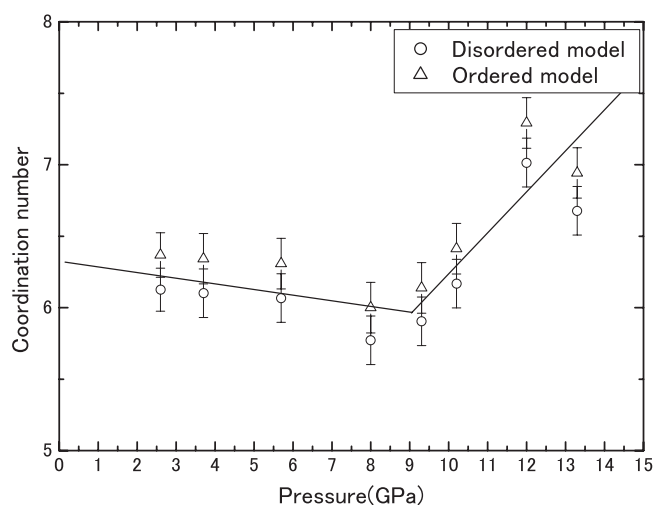
Figure 5. Coordination numbers for liquid InAs at various pressures. The coordination numbers for chemically disordered ($g_{In-In} = g_{As-As} = g_{In-As}$) and ordered models ($g_{In-In} = g_{As-As} = 0$ in the first coordination shell) are shown. The thin line is only a guide for the eye.
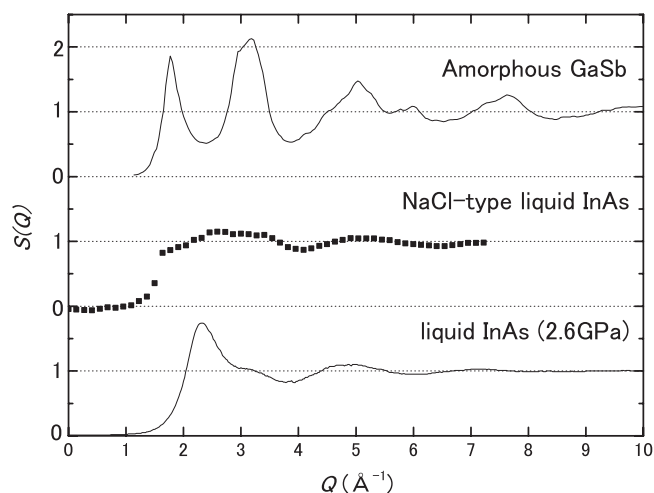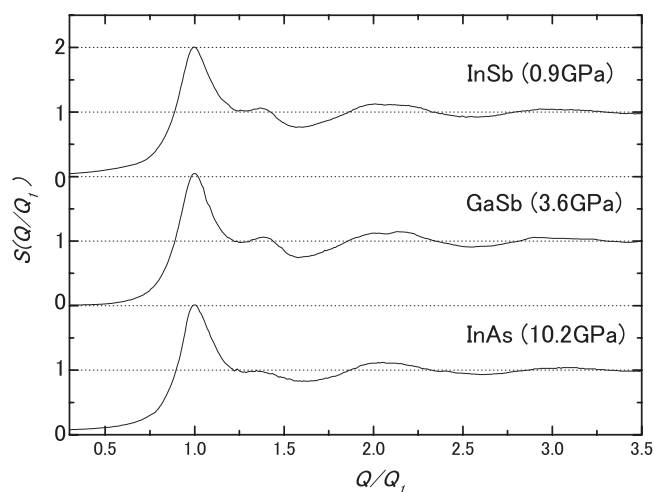

Figure 6. Comparison of $S(Q)$ for liquid InAs with those for the disordered phases with the zinc-blende-like and rock-salt-like local structures. $S(Q)$ for amorphous GaSb is taken from Barkalov *et al* (1996) [22]. $S(Q)$ for liquid InAs with the rock-salt-like local structure is simulated using the partial $S(Q)$s of liquid NaCl [23].

4. Discussion

4.1. Comparison of the structure of liquid InAs with those of the disordered phases consisting of zinc-blende-like and NaCl-like local structures

It is natural to consider the local structure in liquids similar to those in the crystalline states. Therefore, it is likely that the local structures of liquid InAs are similar to the zinc-blende or rock-salt structures. To check this, we compared the experimental $S(Q)$ of liquid InAs with those of disordered materials which have the zinc-blende-like and rock-salt-like local

Figure 7. Comparison of $S(Q)$ for InAs with those for liquid GaSb [5] and liquid InSb [25]. $S(Q)$s with similar Q_2/Q_1 ratios are selected. Each profile is normalized by the position of the first peak.

structures (figure 6). For a disordered material with the zinc-blende-like local structure, the $S(Q)$ of amorphous GaAs [22] is shown. This is because the amorphous solids of the tetrahedrally bonded materials are known to have a continuous random network consisting of tetrahedra [24]. For a disordered material with the rock-salt-like local structure, the $S(Q)$ of liquid InAs which is simulated using the partial $S(Q)$ of liquid NaCl [23] is shown. In the simulation, the differences of the atomic scattering factors of the constituent atoms are taken into account. The comparison reveals that the experimental $S(Q)$ of liquid InAs is significantly different to that for a zinc-blende-type liquid or that for a rock-salt-like liquid in terms of the positions and the heights of the peaks. The coordination number for liquid InAs is also considerably different from that for amorphous InAs ($\approx$3.85 [24]). These findings suggest that liquid InAs can be explained by neither the zinc-blende-type liquid model nor the rock-salt-type liquid model in the pressure region of the present study. This means that the local structure for liquid InAs is considerably different to those of crystalline InAs.

4.2. Comparison of the structure of liquid InAs with those of liquid III–V compounds

The pressure-induced structural changes of liquid III–V compounds have been investigated so far [5–7, 25]. The comparison of the experimental $S(Q)$ of liquid InAs with those for liquid GaSb [5] and liquid InSb [25] is shown in figure 7. Here, profiles with similar Q_2/Q_1 ratios are compared. This is because the profile of each liquid depends on the pressure, and the Q_2/Q_1 ratio is a good parameter for scaling the pressure-induced change. The $S(Q)$ of liquid InAs shows a good agreement with those of liquid GaSb and liquid InSb in terms of the positions and the heights of the peaks as well as the position of the hump. This suggests that the structure of liquid InAs is very close to those of liquid GaSb and liquid InSb. Since the local structures of liquid GaSb and liquid InSb are well described as a mixture of the β-Sn-like and bcc-like local structures [7], the structure of liquid InAs is expected to be describable as the same mixture. Actually, liquid InAs is well described as such a mixture, as is shown later. This supports the picture wherein the local structure of liquid InAs is completely different from those of crystalline InAs.
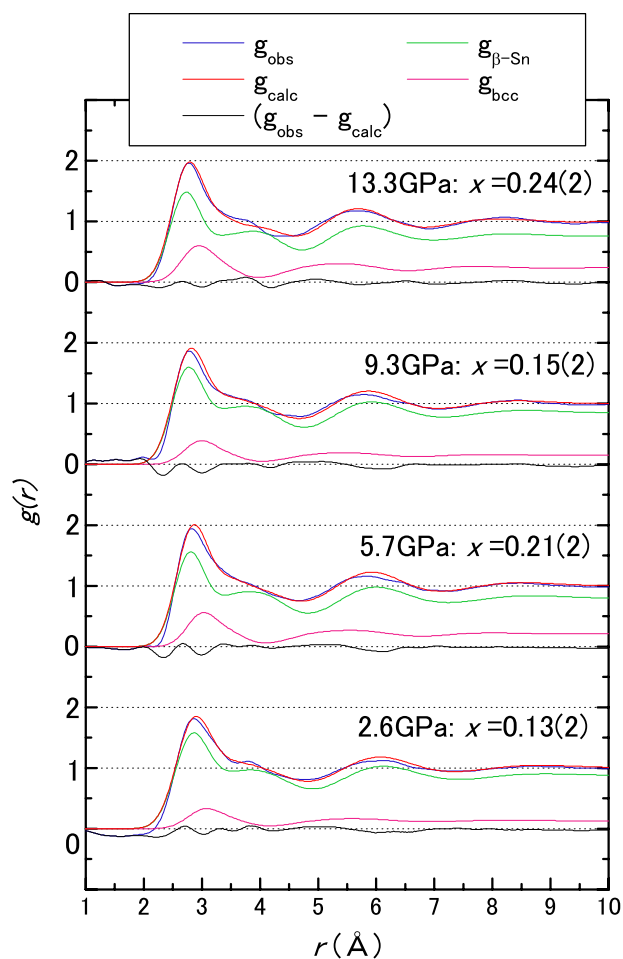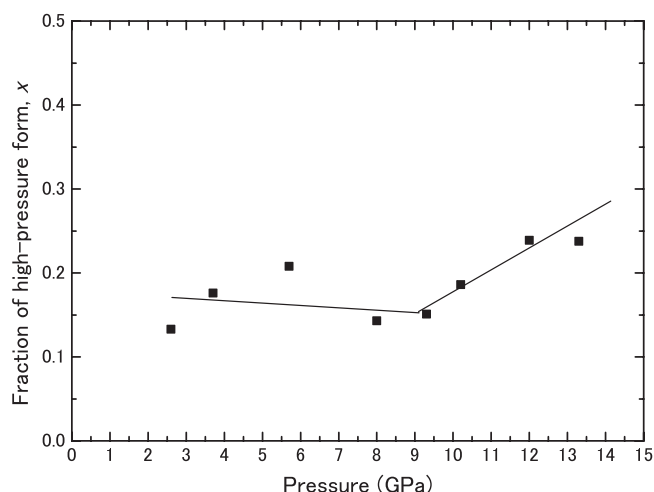
Figure 8. Results of the analyses of the experimental $g(r)$ by a two-species distorted crystalline model [7]. The fraction of the high-pressure form (bcc-like local structure), x, and the uncertainty are shown in the figure.

(This figure is in colour only in the electronic version)

When we consider the effect of the ionic character in the chemical bonds on the local structure of liquids, a lesser effect is observed in the liquid states compared with the crystalline states. Owing to the large ionic character in chemical bonds ($f_i = 0.261$ for GaSb, $f_i = 0.321$ for InSb and $f_i = 0.357$ for InAs [10]), crystalline InAs shows a different pressure-induced change to those of crystalline GaSb and InSb [1]. On the other hand, the results of the present study show that liquid InAs shows the same pressure-induced change as liquid GaSb and InSb in spite of the different ionic character. This clearly shows that the local structures of liquid III–V compounds are less affected by the ionic character in the chemical bonds than those of crystalline III–V compounds.

4.3. Analysis of the local structure

In order to elucidate the local structure of liquid InAs, the experimental $g(r)$ is analysed by the two-species model in conjunction with the distorted crystalline model [7]. In the analyses,

Figure 9. The fraction of the high-pressure form (bcc-like local structure), x, at high pressures. The thin line is only a guide for the eye.

the experimental $g(r)$ is fitted by a linear combination of two $g(r)$s which are simulated for two crystal structures using the distorted crystalline model. Typical results of the analyses are shown in figure 8. The experimental $g(r)$s at high pressures are successfully reproduced by a linear combination of the $g(r)$s simulated for the β-Sn-like and bcc-like structures. This suggests that liquid InAs consists of a mixture of the β-Sn-like and bcc-like local structures. The pressure dependence of the fraction of the high-pressure form (bcc-like local structure), x, is shown in figure 9. Up to 9 GPa, x is almost constant, whereas it gradually increases at the higher pressures. This means that the local structure of liquid InAs does not change markedly up to 9 GPa, and it gradually changes from a low-pressure form (β-Sn-like structure) into a high-pressure form (bcc-like structure) above 9 GPa. The pressure dependence of x is consistent with those of the peak positions in $g(r)$ and the coordination number. That is, in the pressure range where the liquid contracts uniformly, the local structure does not change markedly. On the other hand, in the pressure range where the liquid contracts nonuniformly, the local structure changes from a low-pressure form into a high-pressure one.

When we compare these behaviours with those in the other liquid III–V compounds, such as liquid GaSb and liquid InSb, a marked difference is observed in the pressure range of the structural change. The detailed differences and the reasons for them will be given elsewhere.

5. Conclusion

We have investigated the structure of liquid InAs at pressures up to 13 GPa by means of a synchrotron x-ray diffraction measurement. The main conclusions of this study are summarized as follows.

 (i) The contraction behaviour of liquid InAs changes at about 9 GPa: the liquid contracts almost uniformly below 9 GPa, whereas it contracts nonuniformly above 9 GPa.
 (ii) Local structures which do not appear in the crystalline states are observed in liquid InAs. That is, liquid InAs consists of a mixture of the β-Sn-like local structure (low-pressure form) and the bcc-like one (high-pressure form), rather than the zinc-blende or rock-salt structures which appear in crystalline InAs.

(iii) The local structure does not change markedly up to 9 GPa, whereas it gradually changes from a low-pressure form into a high-pressure one with increasing pressure above 9 GPa.

(iv) The local structure of liquid InAs is basically the same as those of liquid GaSb and liquid InSb in spite of the different ionic character in the chemical bonds. In liquid phases, the pressure-induced structural changes are less affected by the ionic character in the chemical bonds than in the crystalline phases.

Acknowledgments

References

[1] McMahon M I and Nelmes R J 1995 *J. Phys. Chem.* **56** 485 and references therein
[2] Mori T 2000 *Master Thesis* Keio University, submitted
[3] Funamori N and Tsuji K 2002 *Phys. Rev. Lett.* **88** 255508
[4] Koga J and Yonezawa F 2002 *Phys. Rev.* B **66** 12105
[5] Hattori T, Taga N, Takasugi Y, Mori T and Tsuji K 2002 *J. Phys.: Condens. Matter* **14** 10517
[6] Hattori T, Taga N, Takasugi Y, Mori T and Tsuji K 2002 *J. Non-Cryst. Solids* **312–314** 26
[7] Hattori T, Tsuji K, Taga N, Takasugi Y and Mori T 2003 *Phys. Rev.* B **68** 224106
[8] Tsuji K, Hattori T, Mori T, Kinoshita T, Narushima T and Funamori N 2004 *J. Phys.: Condens. Matter* **16** S989
[9] Katayama Y and Inamura Y 2003 *J. Phys.: Condens. Matter* **15** S343
[10] Phillips J C 1970 *Bonds and Bands in Semiconductors* (New York: Academic)
[11] Jamieson C 1963 *Science* **139** 762
[12] Pitt G D and Vyas M K R 1973 *J. Phys. C: Solid State Phys.* **6** 274
[13] Vohra Y K, Weir S T and Ruoff A L 1985 *Phys. Rev.* B **31** 7345
[14] Nelmes R J, McMahon M I, Wright N G, Allan D R and Liu H 1995 *J. Phys. Chem. Solids* **56** 539
[15] Jayaraman A, Klement W Jr and Kennedy G C 1963 *Phys. Rev.* **130** 540
[16] Shimomura O, Utsumi W, Taniguchi T, Kikegawa T and Nagashima T 1992 *High-Pressure Research: Application to Earth and Planetary Sciences* ed Y Syono and M H Manghnani (Washington, DC: American Geophysical Union)
[17] Decker D L 1971 *J. Appl. Phys.* **42** 3239
[18] Faber T E and Ziman J M 1965 *Phil. Mag.* **11** 153
[19] Waseda Y 1980 *Structure of Non-Crystalline Materials* (New York: McGraw-Hill)
[20] Waseda Y, Shinoda K, Sugiyama K and Takeda S 1995 *Japan. J. Appl. Phys.* **34** 4124 and references therein
[21] Mizuki J, Kakinoki K, Misawa M, Fukunaga T and Watanabe N 1993 *J. Phys.: Condens. Matter* **5** 3391
[22] Barkalov O I, Kolesnikov A I, Antonov V E, Ponyatovsky E G, Dahlborg U, Dahlborg M and Hannon A 1996 *Phys. Status Solidi* b **198** 491
[23] Biggin S and Enderby J E 1982 *J. Phys. C: Solid State Phys.* **15** L305
[24] Shevchik N J 1973 *Phys. Rev. Lett.* **12** 1245
[25] Hattori T, Tsuji K, Taga N, Takasugi Y and Mori T 2004 in preparation